

Novel Photoemission Approach to Hot-Electron Transport in Semiconductors

J. Peretti, H.-J. Drouhin, and D. Paget

Laboratoire de Physique de la Matière Condensée, Ecole Polytechnique, 91128 Palaiseau, France

(Received 3 October 1989)

We have performed high-resolution energy analysis of the near-band-gap photoemission of a *p*-type InP/Ag Schottky diode under electrical bias. This original technique brings direct information on high-electric-field electron transport in semiconductors. From our experimental data, using simple models, we estimate characteristic phonon-emission times in an energy range which spans the whole first conduction band, and we evidence an efficient Γ_6 - X_6 intervalley transfer.

PACS numbers: 79.60.Eq, 72.10.Di, 72.20.Ht, 73.30.+y

For a long time, hot-electron transport in semiconductors has been a domain of active research, stimulated by technological challenges. Here we demonstrate that the precise knowledge of the energy distribution curves (EDC's) of the electrons *photoemitted in vacuum* from a low-electron-affinity structure *under electrical bias* is a decisive advantage for the study of these phenomena. Attempts to use field-assisted photoemission techniques were tried many years ago but led to featureless EDC's.¹ Recently, ballistic electron transport has been investigated in internal-emission experiments using hot-electron spectrometers, a closely related technique.²

In our experiment, the sample is a Ag/InP Schottky diode, prepared *in situ*. The detailed technical procedure is described in Ref. 3 and here we just summarize the main points. A (100) InP crystal (*p* doped, $1.2 \times 10^{16} \text{ cm}^{-3}$), chemically etched, is introduced under neutral atmosphere into an ultrahigh-vacuum chamber where it is heat cleaned at about 350°C. The 100-Å-thick Ag layer is evaporated on the clean InP surface (pressure $< 1 \times 10^{-10}$ Torr, evaporation rate $\approx 1 \text{ Å/s}$, sample temperature $\approx 300 \text{ K}$). Such a thin Ag layer is electrically continuous, and semitransparent to near-infrared and visible light as well as to low-energy electrons. The metal surface work function is then lowered by Cs and O₂ coadsorption. All the measurements reported here are performed at 120 K. Near-band-gap light excitation of the semiconductor (energy $h\nu = 1.46 \text{ eV}$) promotes electrons of small kinetic energy ϵ_{ex} (45 meV) in the conduction band (CB) of the bulk solid. Prior to emission into vacuum, these electrons are injected into the band-bending (BB) region towards the surface. There they are heated in the electric field, defined by maintaining a constant voltage between a back electrical contact and the Ag layer. We perform the energy analysis of the photoemitted electrons with a resolution of 20 meV for different bias voltages, using a home-built electron spectrometer in the constant-energy mode, i.e., scanning the sample potential.⁴ We have very carefully modeled our structure, taking into account a rectifying back contact, the Ag/InP diode (with its induced photovoltage), and a parasitic resistance (Fig. 1, inset). From the fit of the current-voltage characteristics of the structure in the dark and under illumination, we have determined the

electrical bias V actually applied to the Ag/InP diode with an accuracy better than the energy resolution. The calculation, lengthy but straightforward, makes use of the standard parameters of Schottky diodes. The barrier height at the Ag/InP interface (0.78 eV) was measured using the photoelectric method. When $V=0$, this corresponds to a BB amplitude $eV_B = 0.72 \text{ eV}$ ($-e$ is the electron charge). In a parabolic BB, the energy of the bottom of the CB versus position, referred to the bottom of the CB in the bulk, is $\epsilon_c(z) = -eV_B(z/w_0)^2$, where z is the abscissa measured along the normal to the surface taking the origin at the bulk/BB interface and w_0 the BB width for $V=0$ (2900 Å in our case). The BB width at bias V is $w = w_0[(V + V_B)/V_B]^{1/2}$. Because an increase of the reverse bias increases the BB width without altering its shape, one can alternatively consider that the EDC's measured at different bias voltages give an insight into the evolution of the EDC with distance in the BB (Fig. 1).

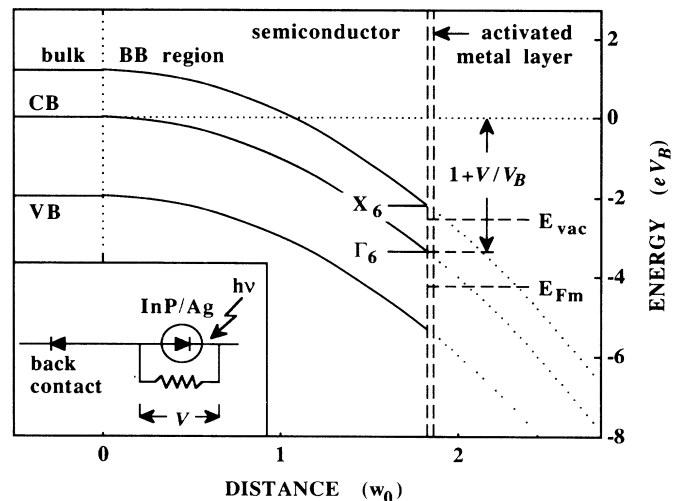


FIG. 1. Band diagram in the BB region showing the valence-band (VB) maximum, the CB minimum, and the X secondary minima of the first CB. The parabolas are drawn up to an arbitrary distance to illustrate that a change in bias potential acts as a displacement of the surface. The metal Fermi level (E_{Fm}) and the vacuum level (E_{vac}) are pinned to the surface-band positions. Inset: Electrical equivalent circuit.

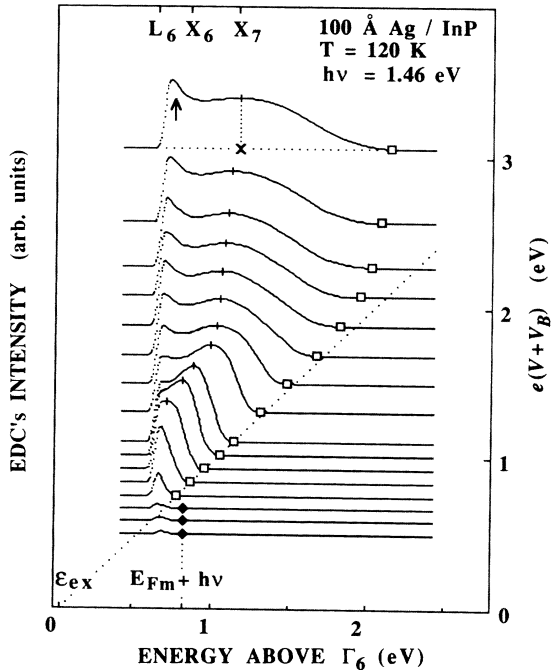


FIG. 2. EDC's at different bias potentials. Electron energy is referred to Γ_6 , the bottom of the CB at the Ag/InP interface. The positions of the relevant conduction-band minima at the interface are indicated on the upper horizontal axis. The curves are normalized so that their area is proportional to the total emitted current. On the vertical scale (right), they are shifted by the BB amplitude, $e(V+V_B)$. The symbols \square and \times refer respectively to the EDC high-energy edge and to the main-peak maximum (indicated by a vertical bar). The low-energy contribution (\uparrow), due to electrons partially relaxed near the Ag/InP interface, is not considered in the discussion. The equation of the dotted straight line is $\epsilon = \epsilon_{ex} + e(V+V_B)$. The high-energy edge of the three lowest EDC's (\blacklozenge) corresponds to electrons excited from the Ag Fermi level.

EDC's of field-assisted photoemission are shown in Fig. 2. At very low bias, the small photoemission current essentially originates from the Ag layer and provides an absolute energy reference. Applying a sizable reverse bias allows electron emission from the semiconductor, which strongly improves the photoemission yield ($\sim 0.4\%$ at $V+V_B \approx 3$ V), and produces spectacular modifications of the EDC's. Different features can be observed on these curves or, as in Ref. 4, on their derivatives which are not reproduced here. For the analysis, we draw the field-assisted structure diagram (Fig. 3), which presents the location of EDC structures versus the BB amplitude $e(V+V_B)$ and is analogous to the usual photoemission structure diagram.⁴ We shall propose models based on order-of-magnitude calculations and, in our conditions (low temperature, low doping level, low electron density), we only take into account the dominant scattering mechanism which is phonon emission.⁵ Here, we only discuss (i) the high-energy edge (\square) and

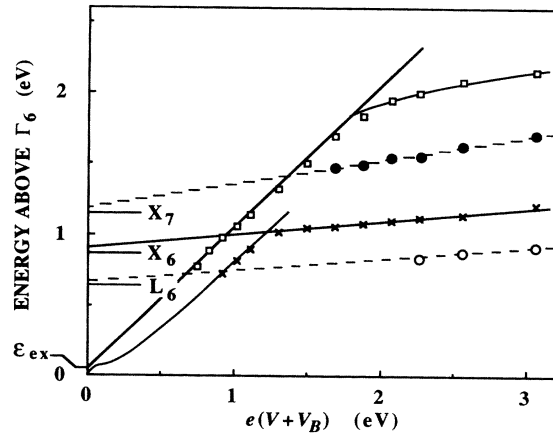


FIG. 3. Field-assisted structure diagram. \square : high-energy end; \times : main-peak maximum. The solid lines are the fits discussed in the text. The symbols \circ and \bullet correspond to features only observed on the EDC derivatives and respectively attributed to the L_6 and X_7 valleys; the dashed lines show that the model given for the X_6 structure also accounts for their variation.

(ii) the maximum of the main photoemission peak (\times).
 (i) The maximum possible electron kinetic energy at the surface, for ballistic electrons, is $\epsilon = \epsilon_{ex} + e(V+V_B)$. We indeed observe this linear variation of the high-energy edge position for $V+V_B \leq 1.70$ V. Saturation seems to occur at an energy of about 2.15 eV, a value larger than the energy width of the first CB. To interpret this fact, note that the electron energy gain is maximum in the [100] direction, parallel to the electric field. In this direction, the electrons should attain a higher-band maximum where their group velocity becomes zero. Near that point, the energy loss per unit length becomes so important that they cannot actually reach it. In a one-dimensional model, assuming that electrons have a stationary energy at each point of the BB, we can write the energy balance:

$$d\epsilon/dt = eE(z)v - \hbar\omega/\tau = 0, \quad (1)$$

where ϵ is the electron kinetic energy, v the electron group velocity, $\hbar\omega$ the typical energy loss in the overall collision time τ , and $E(z)$ the modulus of the electric field. In this energy range, we consider that τ varies slowly enough with ϵ to be taken as a constant. Assuming a parabolic dispersion of the energy band near a maximum at energy ϵ_0 and along the normal to the surface, we get at emission

$$\epsilon = \epsilon_0 - (m^*/2)[\hbar\omega/eE(w_0)\tau]^2 V_B/(V+V_B), \quad (2)$$

where m^* is the effective mass component normal to the surface. Equation (2) fits very well the experimental data for $V+V_B \geq 2$ V and yields $\epsilon_0 = 2.58$ eV. This energy indeed corresponds to an extremum of the second CB in the [100] direction.⁶ Evidence that electrons are transferred there is supported by the observation of a

high-energy feature in the EDC derivatives that we attribute to the second CB minimum X_7 . Taking $\hbar\omega = 40$ meV, a typical phonon energy,⁷ and $m^* \approx 0.2m_0$ (m_0 is the free electron mass),⁶ we deduce $\tau \approx 5$ fs.

(ii) The electrons initially thermalized at the bottom of the CB in the bulk are subsequently heated in the BB region. The energy position of the peak varies linearly versus $e(V+V_B)$ with a slope almost equal to unity when $0.92 \text{ V} \leq V+V_B \leq 1.24 \text{ V}$. Below 0.92 V, the peak cannot be observed as it should lie under the vacuum level. Above 1.24 V it becomes broader and its position still varies linearly, with a slope as small as 0.1.

Low bias ($V+V_B \leq 1.24 \text{ V}$).—Energy losses mainly occur by emission of polar optical phonons of energy $\hbar\omega_{\text{op}}$. The collision time τ_{op} varies with ϵ (for $\epsilon \geq \hbar\omega_{\text{op}}$) like⁵

$$\tau_{\text{op}}(\epsilon) = \tau_0(\epsilon/\hbar\omega_{\text{op}})^{1/2}/\sinh^{-1}[(\epsilon/\hbar\omega_{\text{op}}) - 1]^{1/2}, \quad (3)$$

where τ_0 is a characteristic time constant. The electron kinetic energy remains small as long as the energy gain from the electric field in the electron mean free path λ remains smaller than the energy loss, i.e., $eE\lambda < \hbar\omega_{\text{op}}$. Beyond that point, because the efficiency of this relaxation process decreases with increasing energy, the transport becomes quasiballistic, which is experimentally observed when $0.92 \text{ V} \leq V+V_B \leq 1.24 \text{ V}$. Extrapolating this line to zero kinetic energy shows that quasiballistic transport should start approximately from $V+V_B = 0.15 \text{ V}$. This yields $\lambda \approx 400 \text{ \AA}$, i.e., a collision time of the order of 70 fs. As optical-phonon emission favors forward scattering, we have performed a numerical one-dimensional fit of the transport through the BB region, drawn in Fig. 3. This leads to the value $\tau_0 \approx 35$ fs.

Large bias.—During their quasiballistic transport, the electrons have gained enough energy to be transferred into side valleys by emission phonons. There, intervalley scattering in the equivalent valleys is a very efficient energy and momentum relaxation mechanism. We base our calculation on the two following assumptions: at each point of the BB the transport is almost stationary; the drift velocity is small compared to the electron velocities. The energy gain in the time τ_{iv} between two collisions, after first averaging over the electron velocities in a specified valley, then over the equivalent valleys of the first conduction band (L_6 or X_6), is

$$\Delta\epsilon \approx \frac{1}{2} (e\tau_{\text{iv}})^2 E^2 / m_c. \quad (4)$$

The conduction equivalent mass m_c has the usual definition, $m_c^{-1} = \frac{1}{3} (2/m_t + 1/m_l)$, where m_t (m_l) is the transverse (longitudinal) effective mass. For scattering between equivalent valleys, the mean collision time for phonon emission can be written as⁵

$$\tau_{\text{iv}} = \tau_1(\hbar\omega_{\text{iv}})^{1/2}/(\epsilon - \hbar\omega_{\text{iv}})^{1/2}, \quad (5)$$

where τ_1 is again a characteristic time constant and $\hbar\omega_{\text{iv}} \approx 40$ meV is the intervalley phonon energy. Substi-

tuting Eq. (5) in Eq. (4) for $\Delta\epsilon = \hbar\omega_{\text{iv}}$, we obtain the mean electron kinetic energy, so that at emission,

$$\epsilon \approx \tau_1^2 (2eV_B/m_c \omega_{\text{iv}}^2) e(V+V_B) + \hbar\omega_{\text{iv}}. \quad (6)$$

Equation (6) predicts a linear variation of ϵ vs $V+V_B$, which is experimentally observed. The corresponding straight line is expected to extrapolate for $V+V_B = 0$ at the energy of the side valleys, augmented by $\hbar\omega_{\text{iv}}$, and so, we find that they are located at 0.87 eV above Γ_6 . However, in the literature the positions of the side valleys are not well established and in order to determine them, we performed photoemission experiments on a highly p -doped InP sample ($5 \times 10^{18} \text{ cm}^{-3}$), using the method exposed in Ref. 4. Assuming the usual Γ_6 - L_6 - X_6 ordering, we measure Γ_6 - L_6 , Γ_6 - X_6 , and Γ_6 - X_7 spacings respectively equal to 0.64, 0.87, and 1.15 eV. We conclude that the observed transfer occurs from the Γ_6 to the X_6 valleys. The identification in the field-assisted experiment is again supported by the observation of a small but reproducible lower-energy feature in the EDC derivatives that we attribute to the L_6 valleys. From the slope of ϵ vs $V+V_B$ and taking $m_t \approx 0.3m_0$, $m_l \approx 1.2m_0$ deduced from Ref. 6, we estimate $\tau_1 \approx 100$ fs. Now, the transfer can only occur when the electron energy exceeds the X_6 energy by $\hbar\omega_{\Gamma-X}$, the relevant phonon energy, which corresponds to $V+V_B = 1.12 \text{ V}$. As seen in Fig. 3, an increase of $V+V_B$ from 1.12 to 1.24 V is required to complete it (when the slope of the peak variation versus BB amplitude has dropped from 1 to 0.1). Converting these voltages into BB widths allows us to determine a Γ_6 - X_6 transfer mean free path equal to 200 \AA , i.e., a transfer time $\tau_{\Gamma-X} \approx 20$ fs.

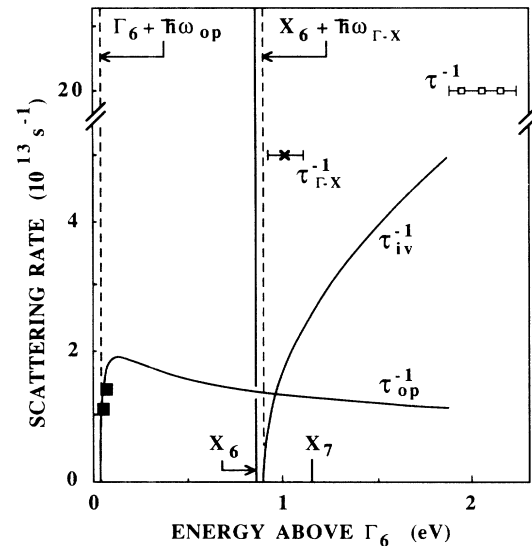


FIG. 4. Scattering rates in the CB band, calculated from the experimental data, for polar optical-phonon emission (τ_{op}^{-1} ; ■, qualitative estimation), Γ_6 - X_6 scattering ($\tau_{\Gamma-X}^{-1}$), X_6 intervalley scattering (τ_{iv}^{-1}), and scattering at the highest energy, in the X_7 valleys (τ^{-1}).

We have presented a new technique which is an accurate way to visualize the evolution of an EDC in a high electric field. Because particular points of physical significance can be precisely followed as a function of bias, a simple analysis provides a quantitative understanding of the dominant mechanisms. So we obtain the characteristic collision times governing energy relaxation as well as intervalley transfer (Fig. 4). It is shown that, when energetically possible, a very efficient transfer occurs from the Γ_6 to the X_6 valleys, which clearly favors the three-valley (Γ_6 - L_6 - X_6) transport models. Today the parameters for hot-electron transport in InP are not well known. Our data are consistent with scattering rates often quoted for GaAs (we obtain intervalley coupling constants $D_{\Gamma X}$ and D_{XX} of about 1×10^9 eV/cm), although the subject remains controversial.⁸ Such information is key to the understanding of ultrafast electron devices and the present method could also be a valuable tool to test the occurrence of Bloch oscillations.

We thank Ph. Bréchet, C. Hermann, G. Lampel, and Y. Lassailly for a critical reading of the manuscript. H.-J.D. and J.P. are grateful to J.-N. Chazalviel for many fruitful discussions. H.-J.D. is a member of the Direction des Recherches, Etudes et Techniques de la

Délégation Générale de l'Armement (D.R.E.T.). This work was performed under Contract No. D.R.E.T. 87-224.

¹T. Itoh, J. Appl. Phys. **41**, 1951 (1970).

²P. H. Beton, A. P. Long, and M. J. Kelly, J. Appl. Phys. **65**, 3076 (1989), and references therein.

³H.-J. Drouhin, D. Paget, and J. Peretti, in *Proceedings of the Tenth European Conference on Surface Sciences, Bologna, Italy, 1988*, edited by C. M. Bertoni, F. Manghi, and U. Valbusa [Surf. Sci. **211/212**, 593 (1989)].

⁴H.-J. Drouhin, C. Hermann, and G. Lampel, Phys. Rev. B **31**, 3859 (1985); **31**, 3872 (1985).

⁵E. M. Conwell, in *High-Field Transport in Semiconductors*, edited by F. Seitz, D. Turnbull, and H. Ehrenreich, Solid State Physics Suppl. 9 (Academic, New York, 1967).

⁶J.-N. Chazalviel (private communication), band structure calculated after M. L. Cohen and T. K. Bergstresser [Phys. Rev. **141**, 789 (1966)].

⁷E. Bedel, G. Landa, R. Carles, J.-P. Redoulès, and J.-B. Renucci, J. Phys. C **19**, 1471 (1986).

⁸R. G. Ulbrich, J. A. Kash, and J. C. Tsang, Phys. Rev. Lett. **62**, 949 (1989).